COMPUTATION FLUID DYNAMIC MODELING OF ROCKET BASED COMBINED CYCLE ENGINE FLOWFIELDS

Russell L. Daines* and Charles L. Merkle[†]

Propulsion Engineering Research Center

Department of Mechanical Engineering

The Pennsylvania State University

SUMMARY

Computational Fluid Dynamic techniques are used to study the flowfield of a fixed geometry Rocket Based Combined Cycle engine operating in rocket ejector mode. Heat addition resulting from the combustion of injected fuel causes the subsonic engine flow to choke and go supersonic in the slightly divergent combustor-mixer section. Reacting flow computations are undertaken to predict the characteristics of solutions where the heat addition is determined by the flowfield. Here, adaptive gridding is used to improve resolution in the shear layers. Results show that the sonic speed is reached in the unheated portions of the flow first, while the heated portions become supersonic later. Comparison with results from another code show reasonable agreement. The coupled solutions show that the character of the combustion-based thermal choking phenomenon can be controlled reasonably well such that there is opportunity to optimize the length and expansion ratio of the combustor-mixer.

INTRODUCTION

The use of multiple types of propulsion cycles is necessary for many hypersonic missions. The present paper addresses some of the flowfield characteristics that are encountered in a combined cycle concept for space launch that is based upon using a rocket engine as the fundamental element [1, 2]. This so-called Rocket Based Combined Cycle (RBCC) propulsion system is of interest for both single-stage-to-orbit (SSTO) and two-stage-to-orbit (TSTO) missions. A key feature is that it allows flight from take-off to orbit with a fixed geometry flow path.

An RBCC propulsion system is comprised of a rocket engine inside an air breathing engine as shown in Fig. 1. Both engines are integrated to operate as a single unit. The RBCC engine has the advantages of lift-off with pure rocket thrust, coupled with the ability to use inducted air as an oxidizer at lower altitudes, pure ram/scramjet performance at higher altitudes, after which it switches back to all rocket thrust after the vehicle is outside the atmosphere. This capability for capturing the oxidizer decreases the amount of stored oxidizer that is required which reduces take-off weight. Integrating the rocket and the air breathing engine also provides synergistic benefits that would not occur for the two units operating separately.

The ejector scramjet (ESJ) version of an RBCC engine operates in four modes: rocket ejector, ramjet, scramjet, and all-rocket mode. Each mode is used in the flight-speed regime where it is most efficient. A

---

*Graduate Research Assistant

[†]Distinguished Alumni Professor

major feature of the ESJ engine is that it operates with a fixed geometry flow path that provides a reduction in both the weight and complexity of the engine system as compared to a variable area flow path. In this fixed geometry flow path, the flow is thermally choked and accelerated supersonically by means of heat addition in a continuously diverging passage rather than a typical converging-diverging nozzle. Extensive research was conducted on rocket based combined cycle engines during the mid-1960's [3, 4], including the development and testing of both hydrogen- and hydrocarbon-fueled engines.

SOLUTION TECHNIQUE

The Favre-averaged, Navier-Stokes equations are solved in this modeling effort. To model the hydrogen-air reactions, an eighteen step, nine species reaction model is used. The specific heat, viscosity, and thermal conductivity of each species are calculated from fourth order polynomial curve fits. The binary diffusivity is calculated using Chapman-Enskog theory and the Lennard-Jones (6-12) potential. Mixture properties are determined using Wilke's mixing rule and appropriate averaging of binary diffusivities [5]. The q-ω turbulence model of Coakley [6] was also used. The temporal discretization of the Navier-Stokes equations is accomplished by means of an explicit, four-stage Runge-Kutta procedure, with the source terms in the species and turbulence equations being treated in a point-wise implicit manner to enhance numerical stability and convergence [7].

PROBLEM DESCRIPTION

The focus of the present paper is on modeling the mixing, combustion, and thermal choking processes in the diverging combustor of an RBCC engine operating in rocket ejector mode. The geometrical configuration is based on the axisymmetric ESJ engine of Congelliere et al. [3] and includes a slightly diverging "mixer" whose wall divergence angle is 0.5°, followed by a "nozzle" of divergence angle 1.75°. The end of the mixer and the beginning of the nozzle is defined as the point where the wall divergence angle increases. The computational domain includes the fuel injection, mixing, and combustion in the mixer and extends past the thermal choke point into the supersonic portion of the nozzle.

The upstream end of the computational domain corresponds to the location of the annular fuel injectors when the engine is in rocket ejector mode and represents the plane at which the fuel and oxidizer begin to mix. For clarity, references to mixer length will refer to the distance from this injection plane to the location where the duct wall angle changes. This length is varied parametrically, starting from a 45 cm base length, but for all computations, the combined length of the mixer and nozzle is 1 m. The inlet radius of the mixer is 6.35 cm. The oxidizer flow entering the mixer is assumed to be a well-mixed combination of air and completely combusted rocket exhaust. For the base case, the mass flow rate is set to the experimentally measured mass flow rate for a simulated free stream Mach number of 0.8. The static temperature is set at 1500 K. The computations are done for engine operation at the stoichiometric mixture ratio. Solutions are obtained on a 201x120 grid.

Multi-species chemically reacting axisymmetric flow results are presented. The heat addition to the flow results from the mixing and combustion of fuel with the subsonic air stream coming from the mixer. This causes the heat addition and flowfield to be closely coupled, resulting in thermal choking that is dependent on the characteristics of the flow. A more detailed discussion of the results and comparisons with Congelliere's experimental measurements [3] are presented elsewhere [8].

183

RESULTS AND DISCUSSION

Representative results for the Mach number in the ESJ base case described above are given in Fig. 2. These results include both full flowfield contours and radial profiles at several axial locations. Specifically, profiles are shown for the mixer inlet (Plane A; $x/L = 0$.) and mid-plane (Plane B; $x/L = 0.23$), the end of the mixer and beginning of the nozzle (Plane C; $x/L = 0.45$), and for planes 75% (Plane D; $x/l = 0.85$) and 100% (Plane E; $x/L = 1.0$) of the way through the nozzle. The radial location in all profile plots is scaled by the local radius. For the solutions presented below the gaseous hydrogen is injected at 1100 K.

The Mach number contours in Fig. 2a show the two annular fuel streams at the mixer inlet. Reaction zones form on both sides of each fuel stream. The temperature in these reaction zones increases rapidly, while the air between the fuel streams remain at a relatively constant temperature. The Figure shows a more rapid initial increase in Mach number in the unheated flow than in the reacting flow. This difference, however, diminishes somewhat as the flow nears the sonic point, although the unheated flow still reaches Mach one at an axial location slightly upstream of the heated flow. The flow in the reaction region reaches the sonic velocity very near the mixer exit, where the wall angle increases. As the flow passes through the sonic point, it continues to accelerate to supersonic velocities. Mixing continues as the flow moves toward the exit, so that the flow Mach number is quite uniform at the nozzle exit except for a small region near the centerline where the flow is traveling at a higher Mach number. This is caused by the lower sonic speed at the centerline.

To complement the comparisons to experimental measurements refered to above and to further verify the predictions of the Runge-Kutta code, we compare the present predictions with those generated by the Finite Difference Navier Stokes (FDNS) code developed at NASA Marshall [9], which uses a pressure-based predictor-corrector algorithm. Mach number profiles at the mixer exit and nozzle exit, shown in Fig. 3, show that agreement between the codes is good. At the mixer exit the FDNS code predicts slightly lower Mach numbers near the wall and outer shear layer. At the nozzle exit, the near-wall discrepancy continues. The FDNS code also predicts less mixing in the bulk of the flow, resulting in a less uniform Mach number profile at the nozzle exit. Overall levels and shear region locations are in good agreement.

Grid adaption was applied to the original solution to better cluster the grid in high gradient regions of the flowfield and achieve better resolution of the shear layers without increasing the number of grid points. Here, the Self-Adaptive Grid Code (SAGE) [10] was used to adapt the grid. The Mach number profiles resulting from these two grids at the mixer exit, seen in Fig. 4, show that the adapted grid yields steeper gradients in the shear layers. Also there is a greater difference in the magnitudes of the peaks and troughs on the adapted grid, indicating less numerical diffusion than in the original solution. Finally, a tendency for the Mach number to overshoot near the centerline on the original grid is not present on the adapted grid.

To study the effects of fuel injection location, the combustor flow was calculated for mixer lengths of 15, 45, 65, 80, and 100 cm. The mixer wall angle was 0.5°. At the mixer exit for all but the 100 cm mixer, an additional length of duct was added with a wall angle of 1.75° to form the nozzle and bring the overall duct length to 100 cm. The centerline Mach number profiles for all five geometries are presented in Fig. 5. The axial locations of the centerline sonic point and the mixer exit are proximate for all but the longest mixer. The flow tends to choke at the location where the wall divergence angle increases if significant heat addition is continuing at that axial location. When significant heat addition has ceased prior to the mixer exit, as occurs in the 80 and 100 cm mixers, the location of thermal choking remains unchanged when the

184

mixer length is changed. In these cases, the subsonic flow upstream of the sonic point is not affected by the change in wall angle in the supersonic region. The subsonic flow is increasingly affected as the mixer length is shortened. In the 15 cm mixer, the flow in the subsonic region is significantly different from the flow in longer mixers. In this short mixer, the Mach number increases at a constant rate through the sonic point. In the other cases the Mach number increases more gradually at first then increases rapidly as the flow goes through the transonic regime. The increasing exit area of the ducts as the mixer is shortened and nozzle is lengthened allows the flow to expand more, increasing the exit Mach number.

As the simulated freestream Mach number increased in the experiments of Ref. 3, the mass flow rate into the engine and the stagnation pressure in the engine downstream of the inlet both increased. It should be noted that for all freestream Mach numbers in rocket ejector mode, the air flow was subsonic in the duct downstream of the inlet. Using the measured mass flow rates as inputs, calculations were performed over a range of vehicle flight speeds for a mixer length of 45 cm. Both the specific impulse and the thrust increase with increasing flight speed. The larger air flow rate allows a larger amount of fuel to be injected and burned, adding more energy to the flow. Overall, the Mach number contours for the different freestream Mach numbers do not vary significantly.

The extent of combustion increased with increasing vehicle velocity. This is indicated by an increased stagnation temperature at the mixer exit, shown in Fig. 6. The increased stagnation temperatures at higher freestream Mach numbers indicate a higher level of heat addition to the flow. The higher temperature regions are broader radially for the higher speeds, indicating that the mixing between the fuel and oxidizer is enhanced at these conditions. As the freestream Mach number increases, the air stream mass flow rate increases, so the mass flow rate of hydrogen fuel is also increased to maintain stoichiometric conditions. As this occurs, the velocity ratio between the fuel stream and the oxidizer stream increases. The increased shear velocity causes the flows to mix more rapidly. This trend of increasing combustion efficiency is opposite from the experimental results, which showed an initial decline in combustion efficiency as the freestream Mach number increased.

ACKNOWLEDGEMENTS

REFERENCES

1. Escher, W. and Schnurstein, R., AIAA Paper 93-1944, Monterey, CA, June 1993.
2. Foster, R., Escher, W., and Robinson,J., AIAA Paper 89-2294, Monterey, CA, July 1989.
3. Congelliere, J., Prevatte, N., and Lime, J., Rep. No. AFAPL-TR-67-118, The Marquardt Corp., May 1968
4. Odegaard, E. and Stroup, K., Rep. No. AFAPL-TR-66-49, The Marquardt Corp., October 1966
5. Yu, S., Tsai, Y., and Shuen, J., AIAA Paper 89-0391, Reno, NV, January 1989.
6. Coakley, T., AIAA Paper 83-1693, Danvers, MA, July 1983.
7. Weiss, J., Daines, R., and Merkle, C., AIAA Paper 91-3557, Cleveland, OH, September 1991.
8. Daines, R. and Merkle, C., AIAA Paper 94-3327, Indianapolis, IN, June 1994.
9. Wang, T., Computational Fluid Mechanics J., vol 1, no. 3, October 1992.
10. Davies, C. and Venkatapathy, E., Update to NASA Tech. Memo. 103905, March 1994.
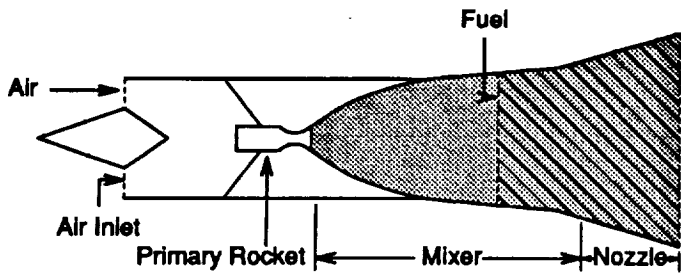
Figure 1: Schematic diagram of a generic RBCC engine. Reaction zone indicated by hatched region.

Figure 3: Radial Mach number profiles at the mixer exit (C) and the nozzle exit (E) from the Runge-Kutta and FDNS codes.
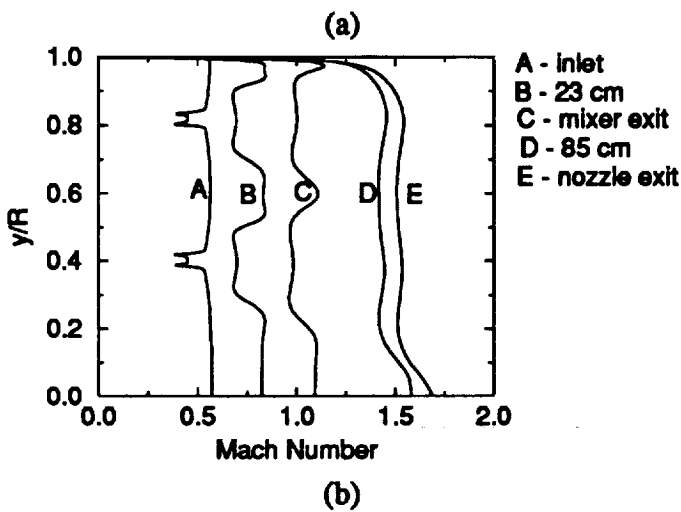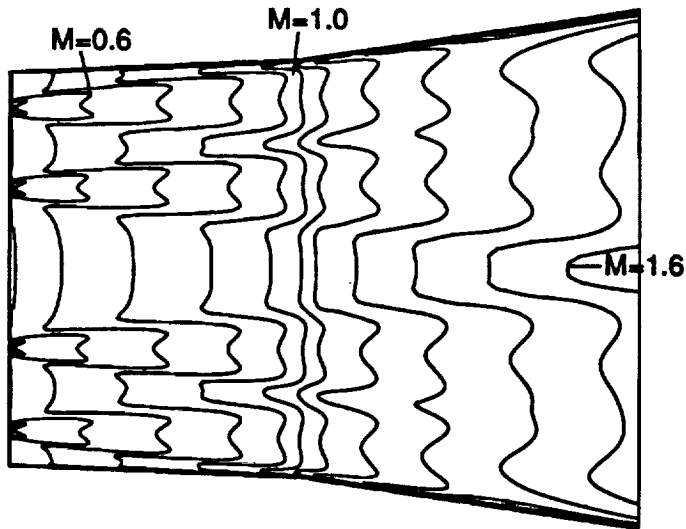

Figure 2: Mach number contours and radial profiles for axisymmetric reacting flow in a duct with a 45 cm mixer. Contour intervals are 0.1. Contour plot is shown here at a 5:1 radial aspect ratio for clarity of details.
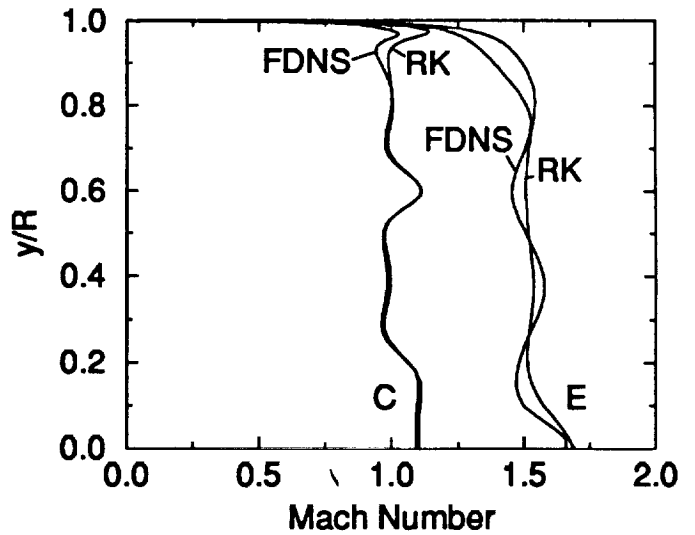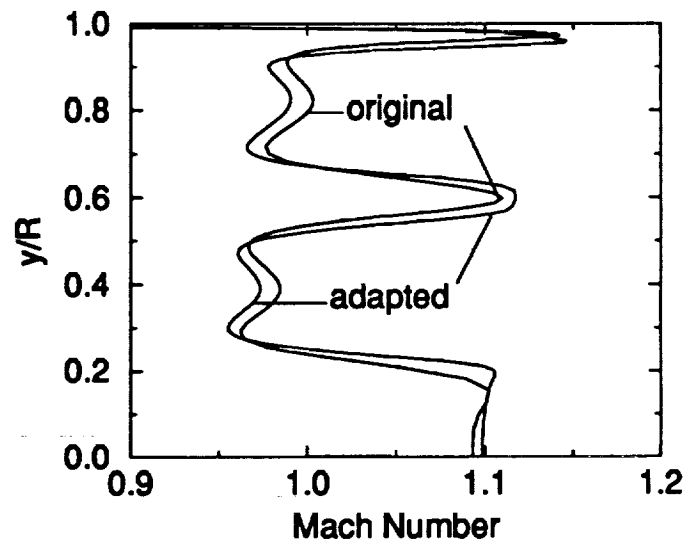

Figure 4: Radial Mach number profiles at the mixer exit on the original and adapted grids.
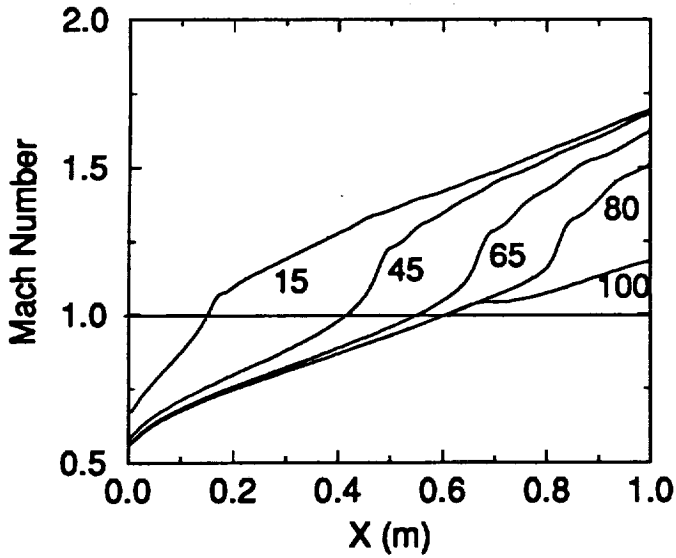
Figure 5: Centerline Mach number profiles for ducts with mixer lengths of 15, 45, 65, 80, and 100 cm. The straight line indicates the sonic point.
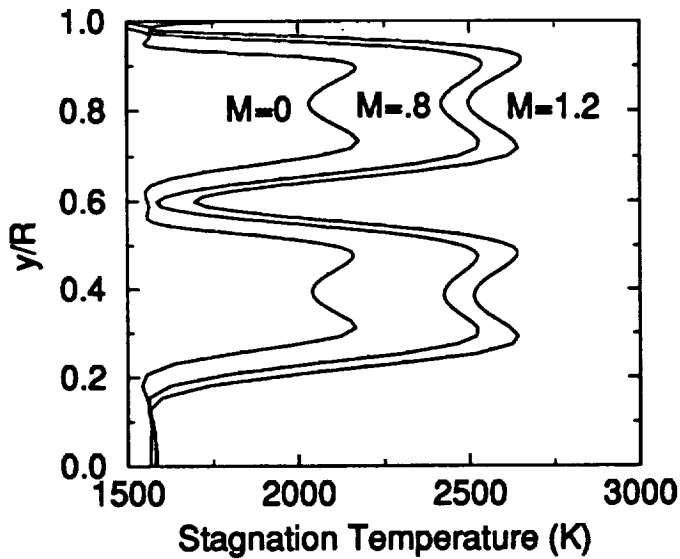

Figure 6: Mixer exit stagnation temperature profiles for varying freestream Mach numbers. Mixer length is 45 cm.